Many-body mechanochemistry: Intramolecular strain in condensed matter chemistry

Brenden W. Hamilton[1] and Alejandro Strachan[2,*]
[1]Theoretical Division, Los Alamos National Laboratory, Los Alamos, New Mexico 87545, USA
[2]School of Materials Engineering and Birck Nanotechnology Center, Purdue University, West Lafayette, Indiana 47907, USA

(Received 6 September 2022; revised 17 May 2023; accepted 11 July 2023; published 25 July 2023)

Molecular strains can greatly alter chemical reactions in covalent systems. Experimental and computational tools designed to characterize this have focused on simple elongation forces. Yet, mechanical loading in condensed matter results in complex, many-body deformations. Hence, we use four-body external potentials designed to reproduce these strains with reactive molecular dynamics. Mimicking these deformations results in significant lowering of activation barriers and different reaction pathways in the energetic material 1,3,5-trinitro-2,4,6-triaminobenzene (TATB) and a lower-energy reaction pathway for isomerization in spiropyran.

DOI: 10.1103/PhysRevMaterials.7.075601

I. INTRODUCTION

Mechanochemistry, the use of mechanical loads to trigger or influence chemistry, can enable otherwise forbidden reactions [1], strengthen polymers without limiting their elongation [2,3], and prompt isomerization reactions in mechanophores [4–9]. Mechanochemistry is also believed to play a role when materials are subjected to extreme dynamical loads such as during planetary collisions [10,11] and shock initiation of explosives [12–15].

Over the last few decades, significant progress has occurred towards an understanding of covalent mechanochemistry in organic and molecular solids [16]. Experiments with exquisite resolution have revealed the strong effect of mechanical forces on chemistry [17,18]. Electronic structure calculations have shown that elongation forces on mechanophores can induce isomerization and ring-opening reactions [4,5,19,20], shown a reduction in strength and distribution of stresses in knotted/entangled polymers [21–24], explored the mechanical stresses in protein folding [25], and assessed the rupture force and electronic properties for extension and scission of metal-organic junctions [26–28]. These types of studies use special-purpose methods to characterize the effect of pairwise external forces on chemistry, including steered molecular dynamics [29–33], constrained geometries simulate external force (CoGEF) [34], and explicit force methods such as force-modified potential-energy surface [20], external force explicitly included [35], and enforced geometry optimization [36].

In general, the understanding of mechanical strains in molecules can be used to assess reaction barriers for thermal activation. The distortion/interaction model [37,38] (or activation-strain model [39]) defines the activation barrier for the reaction as the strain energy needed to deform the molecule to the geometry of the transition state and the interaction energy of the constituent components of the reaction [40]. This helps to define the idea of an activation strain, or the strain needed for a molecule to be able to reach the transition state. While thermal vibrations can cause these distortions to occur stochastically, nonthermal strains due to pressure and material flow can cause these deformations as well [41]. Deformations will not always be along the reaction path to the transition state, but will project onto it by some amount.

To date, computational and experimental studies designed to single out the effects of mechanochemistry have focused on elongation (two-body forces), while most cases of extemporaneous mechanochemistry [15] in condensed matter involve more complex, many-body (MB) deformations. Examples of such MB mechanochemistry (MBMC) include shock-induced chemistry in shear bands [14] and pore collapse [13], the deformation of polymers [4,16,42,43], and organic systems under uniform shear loads such as prebiotic compound formation [10], energetic material decomposition [44], and phase transitions in carbon [45,46]. These material events tend to bend and twist molecules instead of elongate them. While the importance of nonelongation mechanochemistry is incontestable, we currently lack a complete understanding of how specific deformations affect chemical kinetics and reaction paths and the tools to perform such studies. Condensed matter leads to significantly different deformations in molecules than that of single-molecule force spectroscopy, and therefore, condensed matter mechanochemistry must be studied in a way that captures these effects.

In this paper, we utilize a computational approach, many-body steered molecular dynamics (MBsMD), to characterize MBMC. The approach is designed to capture and mimic the conditions experienced in condensed matter via the application of four-body external potentials that affect torsional and out-of-plane deformations to match molecular states measured in condensed matter simulations under relevant conditions. Our approach demonstrates the importance of many-body deformations on the thermal decomposition of 1,3,5-trinitro-2,4,6-triaminobenzene (TATB) and the activation energy of mechanophore isomerization (spiropyran). The former exemplifies a mechanochemically assisted thermal reaction, in which molecular strains accelerate the decomposition reaction. The latter is a case in

*Corresponding author: strachan@purdue.edu

which the reaction is entirely mechanochemical, but involves deformation work applied along different paths. In both examples, the external four-body potentials are designed to match the intramolecular strains observed in independent simulations of deformation in the condensed system. The first example, TATB, using reactive molecular dynamics, shows marked changes in chemical kinetics and decomposition paths that can explain previous inconsistencies in reactions from mechanical and thermal insults [13,14,47]. In the second example, spiropyran, we apply a four-body deformation to torsionally strain the molecule around the spiro atom and use the CoGEF [34] method to load the mechanophore, showing a $\sim 45^\circ$ rotation reduces the energy barrier associated with isomerization by 45%.

II. METHODS

Computational mechanochemistry studies of single-molecule deformations use various techniques to deform systems of interest and explore the evolution of the system as an external force or displacement is increased. However, most approaches cannot readily capture complex many-body molecular distortions observed in condensed matter by utilizing linear strains [14,43,48,49]. To address this gap, we develop MBsMD that uses a four-body external biasing potential to deform molecular groups of interest along torsional and out-of-plane degrees of freedom (DoF). Four-body terms are motivated by our observation of the large molecular distortions observed under shock loading [43] and uniaxial strain. This external biasing potential is implemented in the form of four-body harmonic interatomic potential,

$$E = \tfrac{1}{2}K(\phi_{ijkl} - \phi_o)^2, \tag{1}$$

where ϕ_{ijkl} is either a dihedral angle measuring torsions around the central j bond, or an improper dihedral angle measuring out-of-plane distortions. MBsMD implementation details in LAMMPS [50,51], as well as statistical characterizations of deformed molecules, are available in Secs. S1 and S2 of the Supplemental Material [52]. We apply deformations in independent simulations for a variety of values for the spring constant (K) and target angle (ϕ_o) to parametrically study the effects of each deformation parameter on reaction kinetics, as shown in Sec. S3 of the Supplemental Material (SM) [52].

All simulations use all-atom representations, and molecular dynamics (MD) simulations were performed using LAMMPS [50,51] with a 0.025-fs timestep, integrated with the Verlet scheme under isothermal-isochoric (*NVT*) conditions. The ReaxFF [53] reactive force field was used and partial atomic charges were calculated using the charge-equilibration scheme [54] at every step in the simulations with a tolerance of 1×10^{-6}. While ReaxFF is well parametrized for the materials used here, we note that highly strained systems may not be well defined by the potential. Future work will leverage machine-learning potentials that can be easily retrained to include *ab initio* data on highly strained molecules.

For TATB [see Fig. 1(b)], we used a fully periodic simulation cell with 250 molecules (6000 atoms) in the triclinic crystalline lattice setting of Cady and Larson [55]. Atomic interactions were calculated using the ReaxFF parametrized in Ref. [56] that has previously been used to study the TATB system for shock loading and thermal decomposition [57,58].

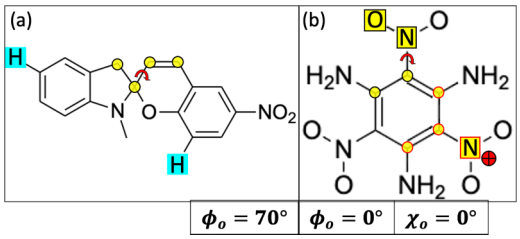

FIG. 1. Spiropyran (a) and TATB (b) molecules. Atoms colored cyan are used as anchor atoms for CoGEF simulations. Atoms colored yellow take part in an external potential deformation. Yellow with a black border corresponds to torsional deformations. Yellow atoms with a red border take part in out-of-plane deformations. For TATB (b) each deformation is separately applied to different decomposition simulations. Angles below molecule panels are equilibrium angles for proper (ϕ) and improper (χ) dihedrals.

Thermal decomposition under the presence of the external potential is simulated by linearly heating the system from 1000 to 3000 K at various rates (from 4 to 40 K/ps) [59] under isochoric conditions. The characteristic reaction time, t_d, defined as the point of maximum internal energy, follows the expected dependence on heating rate (see Sec. S6 of the SM), from which we extracted activation energies.

To mimic the deformations observed in shocked TATB [43], we applied two external potentials in two independent sets of simulations: (i) proper dihedrals of C-C-N-O atoms that control the torsional rotation of the nitro group, and (ii) improper dihedrals of C-C-C-N (nitro group only) that bend the nitro groups away from the plane of the ring, an "out-of-plane" deformation. The external potential is applied simultaneously to all three nitro groups in all 250 molecules, and the system is equilibrated and relaxed for 20 ps at 300 K and 1 atm (*NPT* conditions) under the presence of the external potential to equilibrate the strained system prior heating and decomposition.

For mechanophore simulations, a gas-phase spiropyran molecule (open boundaries) [see Fig. 1(a)] is employed. Atomic forces were calculated with REAXFF, parametrized in Ref. [60]. We employ the CoGEF [34] algorithm, with anchored H atoms, using a constrained structural relaxation via the conjugate gradient method [61] with energy and force tolerances of 1×10^{-4} (percentage) and 1×10^{-6}kcal/molA, respectively. To better explore the underlying energy landscape and avoid local minima, we perform a short, 10-fs, adiabatic (*NVE*) MD simulation prior to each geometry optimization, which improves the predicted reaction pathway; see Sec. 4 of the SM.

We include a four-body potential to control the dihedral angles around the spiro atom and a C atom in the adjacent six-member ring. This is found to be a common deformation in spiropyran + Polymethyl methacrylate (PMMA) condensed matter systems under compression [9]. The equilibrium dihedral angle in the gas phase predicted by ReaxFF is 72°, which compares well to the density-functional theory (DFT) prediction of 77.2° [5]. A spring constant of 50 kcal/mol is used and the target angle is varied from 70° to 25° across independent CoGEF simulations. We determine the energy barrier for isomerization as the difference in total energy (not

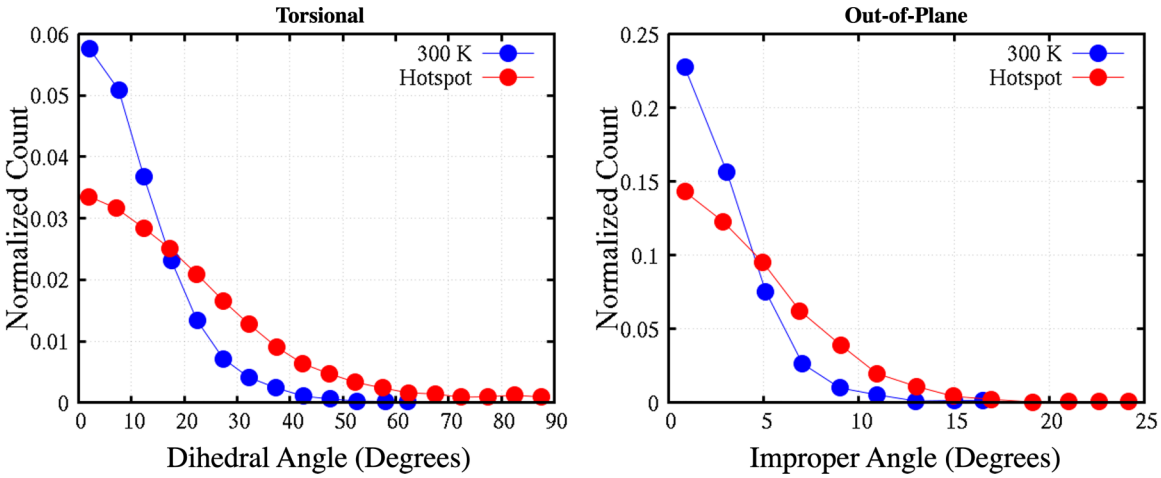

FIG. 2. Distributions of common intramolecular deformations in a shock-induced hotspot [43] compared to a relaxed crystal at 300 K.

including the biasing potential-energy contributions) between the initial configuration and the state just before C–O bond scission is observed. The system was predeformed in regards to the central torsion at 300 K.

III. TATB MECHANOCHEMICALLY ASSISTED THERMAL DECOMPOSITION

When materials experience dynamic mechanical loading, such as during a high-velocity impact, the resulting shock-wave can generate a plethora of ultrafast thermal, mechanical, and chemical processes [62]. These processes are accelerated by energy localization into so-called hotspots. There is increasing evidence from computational studies that hotspots formed under shock loading react at rates significantly faster than equilibrium thermochemistry [13,14]. A possible origin of this increased reactivity is the presence of highly strained and deformed molecules [43,48]. This increase in strain energy in TATB is caused primarily by torsional and out-of-plane deformations of the nitro and amino groups, shown in Fig. 2, and a local amorphization of the material that affects kinetics [63] and heat transport [64].

To assess the influence of these extemporaneous molecular strains on reactivity, we applied four-body biasing potentials to all nitro groups in all TATB molecules in two sets of simulations: torsional-deformation simulations and out-of-plane deformation simulations. Figure 3(a) shows the resulting activation energy associated with decomposition as a function of the average value of the angle (dihedral or out of plane) obtained from a series of simulations with varying external potentials. The green star represents the value for a system with no applied external potential. Both MB strains result in a reduction of the activation energy for decomposition. Yet, we find a significantly larger effect for the out-of-plane bending deformation compared to the torsional deformation, implying a mode-specific effect, which is mostly expected assuming the reaction path and transition state do not change as a result of the deformation. It is interesting to note that the application of MBsMD using angle values close to the equilibrium values results in an increase in the activation energy, as the molecules become more rigid. To further assess the mechanochemical potency of each MB deformation, Fig. 3(b) shows the decrease in activation energy as a function of the strain energy caused by the external MB potential at 300 K. Strain energy is calculated as the REAXFF potential energy of the strained molecule, referenced by the relaxed molecule, i.e., the energy of the external field is not counted. While the out-of-plane deformation of the nitro groups imparts more strain energy, it still has a stronger effect on facilitating the decomposition of TATB given some energy.

We fit these activation barrier results to generate a simple mechanochemical kinetics model with an Arrhenius-like form [65]. In both cases a linear functional form for the change in activation energy from the change in molecular energy works well. This follows the ideas of Hammond's postulate [66] and the Bell-Evans-Polanyi principle [67,68], which show that the difference in reaction barriers of two similar reactions is proportional to the enthalpy of reaction: $E_a = E_o + \alpha \Delta H$, where α is the relative position of the transition state along the reaction coordinate. This also follows the linear trend in activation energy with applied force from Bell [65]: $E_{a_{MC}} = E_{a_o} - Fx$, where the decrease is from the force along some reaction coordinate x. We chose to use the molecular energy increase value in Fig. 3(b) (ΔU_{strain}) and multiply it by a scaling factor that shows how the strain energy projects onto the reaction path. For the torsional deformation, this unitless scaling factor [the slope of the line in Fig. 3(b)] is 0.045. For the out-of-plane deformation, we use a bilinear fit above and below 25 kcal/mol, where this corresponds to a strain-induced conformational change in the molecule, as shown in Sec. S8 of the Supplemental Material [52]. This conformational change also alters the chemical paths, described below. The lower and higher-energy slope values are 0.144 and 0.034, respectively. Section S7 of the SM shows these fits using the deformation angle of Fig. 3(a) [52].

We turn our attention to whether many-body deformations affect the decomposition path, specifically, the primary, initial step. Several initiation mechanisms have been proposed and studied for TATB. Intramolecular hydrogen transfer from the nitro to amino groups is the primary reaction pathway, occurring in nearly 100% of reactions under thermal insults [69] and the majority of initial reactions for shock insults [58].

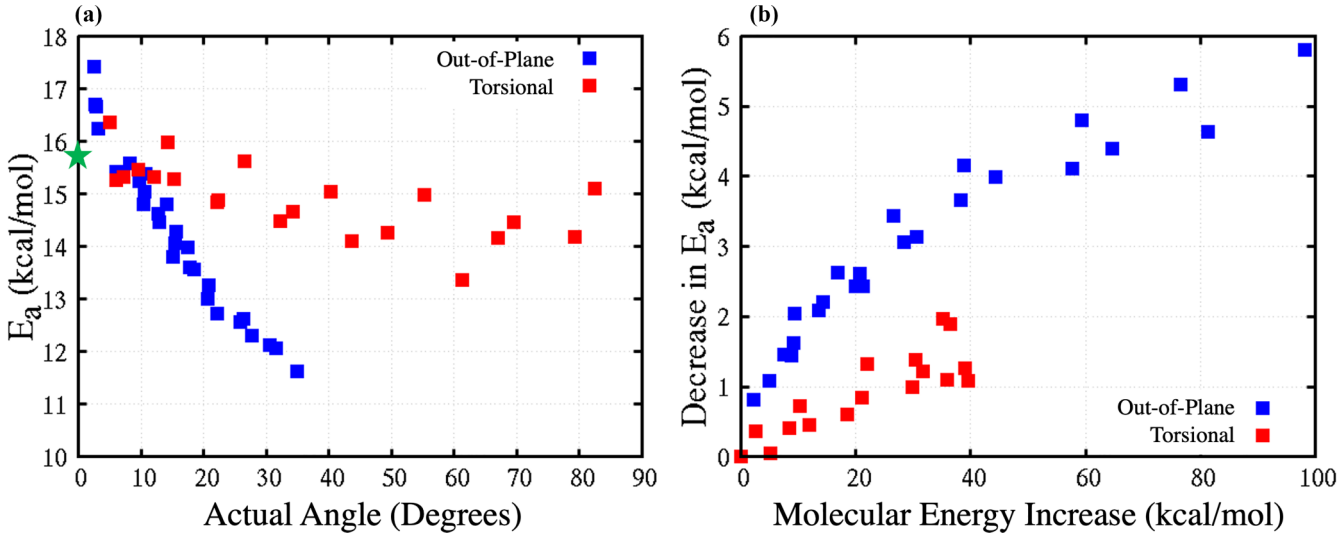

FIG. 3. (a) Activation energies for both types of deformations applied to NO_2 groups. Green star represents unbiased system. The x axis is measured level of deformation at unreacted 300 K state, which is always lower that set angle of biasing potential. (b) Decrease in activation energy compared to undeformed state. The x axis is deformation's rise in potential energy as compared to the 300 K unreacted state.

Intermolecular hydrogen transfer is the main alternative reaction pathway [69] and TATB shear-band chemistry showed an increase of nitro-scission reactions [14].

Our simulation reveals that both molecular strain types have a strong effect on decomposition paths, as shown in Fig. 4. While intramolecular H transfers dominate at low strain, torsional deformations around the C–N (nitro group) bond of over 40° opens a second decomposition path: bimolecular hydrogen transfer. This bimolecular path becomes the primary path for angles above 70°. Interestingly, for angles below the 40° deformation, the amino groups increase their level of deformation as nitro groups deform. Above 40° the amino groups begin to significantly undeform with increasing nitro deformation, i.e., they find that breaking their hydrogen bonds with the nitro groups and relaxing is energetically preferable to deforming alongside the nitro groups, as shown in Sec. S9 of the SM, which corresponds to the onset of the alternate reaction pathway.

For the out-of-plane bending, shown in Fig. 4(b), there is also a change in mechanism for strong enough many-body potentials. Surprisingly, this deformation opens up a different, alternate reaction path: nitro-group scission. The availability of these alternative paths coincides with a conformation change in the TATB. As described in detail in Sec. S8 of the SM, the inner C ring buckles and the nitro and amino groups may more freely rotate (torsional). This structural change causes the change in slope of activation energy vs deformation shown in Fig. 3. Hence, we find that deforming different DoFs in the system results in both different levels of activation barrier reduction and opens different reaction pathway changes.

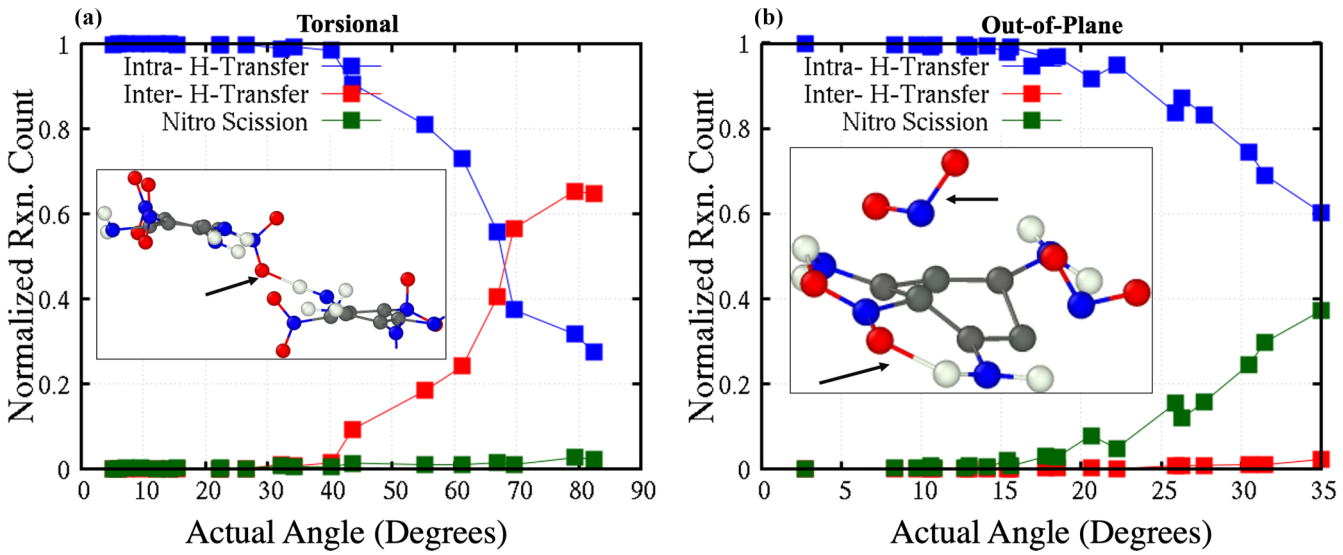

FIG. 4. Percentage of first step reaction pathways for both TATB deformations: torsional (a) and out of plane (b). Inset images are molecular renderings of relevant reactions. Panel (a) shows an intermolecular H transfer; panel (b) shows an intramolecular H transfer (lower arrow) and a nitro scission (upper arrow).

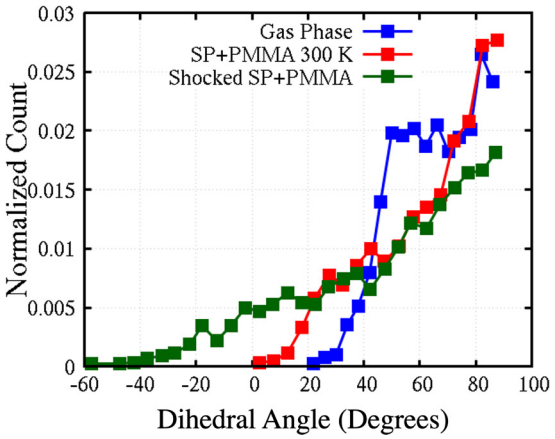

FIG. 5. Distribution of torsional deformations for central dihedral of a gas-phase spiropyran molecule and spiropyran molecules inserted into PMMA chains at 300 K and 1 atm as well as compressed to 40 GPa.

IV. SPIROPYRAN TORSIONAL-DEFORMATION PROMOTED ACTIVATION

Extension of the spiropyran molecule can induce the scission of the C–O bond at the spiro atom through an isomerization reaction, as shown in Ref. [5]. Note that REAXFF overpredicts the DFT barrier to isomerization by roughly 0.5 eV. As was done in prior studies of mechanophores [5,20], we performed CoGEF simulations to characterize this reaction but, in addition to the constraints applied to the anchor H atoms, we applied MBsMD around a central bond. Ten independent CoGEF simulations were performed for each target torsional angle, ranging from 70° to 25°. These mimic deformations seen in a condensed phase spiropyran PMMA copolymer under mechanical loads [9], which show a significant deviation in the central dihedral angle from the equilibrium gas-phase value, as shown in Fig. 5.

Figure 6(a) shows a significant reduction in the energy barrier as the torsional angle is driven away from the equilibrium value of 72°, with a torsional deformation of 45° reducing the energy barrier by 45%. The free-energy difference is obtained from the Jarzynski equality [29], the blue line in Fig. 6(a). The central rotation studied here does not greatly affect the reaction path or product state of the reaction, which is critical in engineering applications of mechanophores. Renderings of the reaction pathway are available in Sec. S4 in the SM, which compares well to predicted isomerization pathways from DFT results [5].

The energy difference in Fig. 6(a) is referenced to the deformed state, but, quite remarkably, MB strains also reduce the total work required for isomerization (referenced to the unstrained system with no MB strain) [see Fig. 6(b)], which is the sum of the pulling work and the work needed to torsionally strain the molecule. The total work needed is also equivalent to the energy rise before reaction, with respect to the relaxed molecular structure. We present this as a "relative total work" where everything is referenced to the case with no torsional strain. This indicates that the MB deformation not only increases the absolute energy of the reagent, but also reduces the energy needed to reach the transition state. Approximately two-thirds of the reduction in the reaction barrier originates from a decrease in the latter. Torsional deformations resulting in dihedral angles approaching 20° (change >50°) result in a small percentage of systems undergoing isomerization without applying a linear strain, at 300 K.

V. CONCLUSIONS

Mechanical loads can cause complex, many-body strains in molecular solids. Such deformations are ubiquitous during dynamical loading and their effect on chemistry is

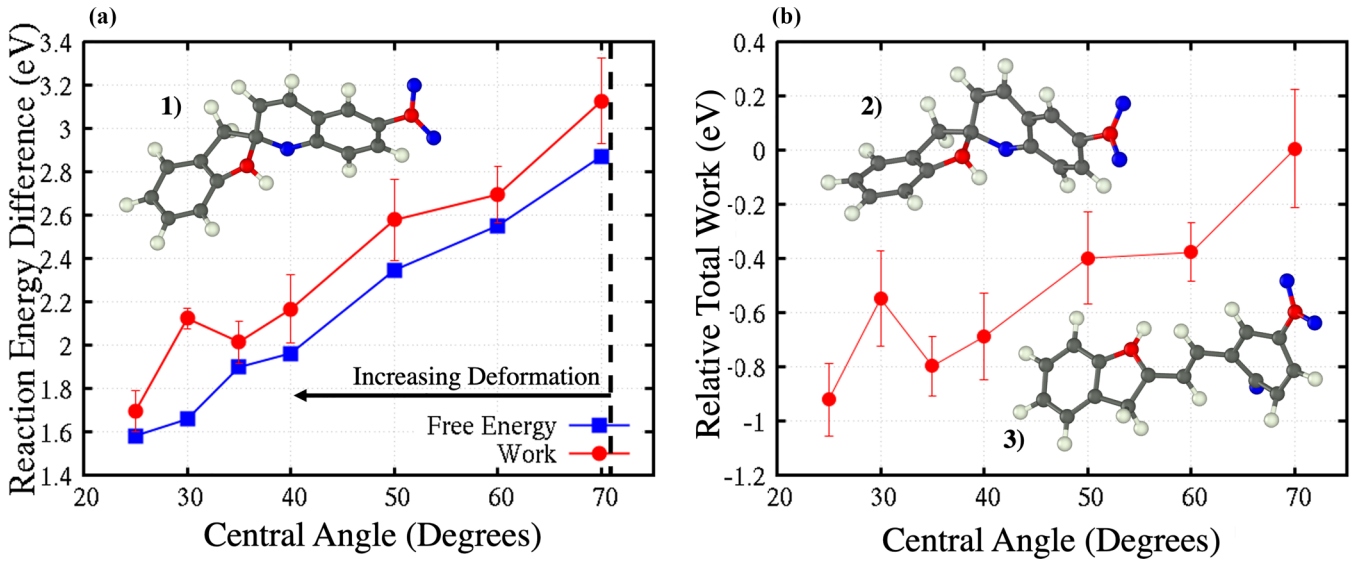

FIG. 6. Reaction energy differences (a) and relative total work (b) for spiropyran isomerization as a function of torsional deformation. Relative total work is pulling work and torsional work done, referenced by value for no torsional deformation. Inset (1) is an undeformed spiropyran, inset (2) is a spiropyran deformed to a 30° state, and inset (3) is a reacted spiropyran. Dashed line in (a) corresponds to undeformed state.

not understood. To fill this gap, we study the effect of four-body molecular strains on condensed matter using reactive MD simulations. This approach captures the complex mechanochemical states experienced in condensed matter chemistry, including shock-induced chemical initiation in high explosives. Our results indicate that many-body strains play an important, sometimes dominant, role in covalent mechanochemistry.

For TATB, MB strains designed to mimic the deformations found during shock loading and pore collapse lead to a significant decrease in activation energy and, quite interestingly, change in the decomposition path. These results explain the increasing evidence of accelerated chemistry in highly deformed areas in shocked explosives and MBsMD will likely be a vital method for developing a predictive understanding of their initiation as well as separating the effects of mechanochemistry from pressure. Additionally, new-generation machine-learning potentials may be tuned for a more accurate description of highly deformed molecular states.

In the isomerization reaction of the mechanophore spiropyran, torsional deformations around the central spiro atom that are induced during compression of a PMMA copolymer, led to a decrease in the energy barrier by 45% for rotations of 45°. Importantly, such intramolecular deformation lowers the absolute energy of the transition-state pathway associated with the activation of the mechanophore as compared to the simple two-body deformations studied to date. These two examples illustrate the pervasiveness of MBMC in condensed matter and the necessity to consider condensed matter effects in mechanochemistry.

Datasets for this work are available publicly through the Materials Data Facility [70].

ACKNOWLEDGMENTS

The authors thank Matthew Kroonblawd for discussions on deformations in TATB and TATB shear-band chemistry. This research was sponsored by the Army Research Laboratory and was accomplished under Cooperative Agreement No. W911NF-20-2-0189. Partial support was received from the U.S. Office of Naval Research, Multidisciplinary University Research Initiatives (MURI) Program, Contract No. N00014-16-1-2557. Program managers included Chad Stoltz and Kenny Lipkowitz.

[1] J. Wang, T. B. Kouznetsova, Z. Niu, M. T. Ong, H. M. Klukovich, A. L. Rheingold, T. J. Martinez, and S. L. Craig, Inducing and quantifying forbidden reactivity with single-molecule polymer mechanochemistry, Nat. Chem. **7**, 323 (2015).

[2] Z. Wang, X. Zheng, T. Ouchi, T. B. Kouznetsova, H. K. Beech, S. Av-Ron, T. Matsuda, B. H. Bowser, S. Wang, J. A. Johnson, J. A. Kalow, B. D. Olsen, J. P. Gong, M. Rubinstein, and S. L. Craig, Toughening hydrogels through force-triggered chemical reactions that lengthen polymer strands, Science **374**, 193 (2021).

[3] A. L. B. Ramirez, Z. S. Kean, J. A. Orlicki, M. Champhekar, S. M. Elsakr, W. E. Krause, and S. L. Craig, Mechanochemical strengthening of a synthetic polymer in response to typically destructive shear forces, Nat. Chem. **5**, 757 (2013).

[4] N. Deneke, M. L. Rencheck, and C. S. Davis, An engineer's introduction to mechanophores, Soft Matter **16**, 6230 (2020).

[5] D. A. Davis, A. Hamilton, J. Yang, L. D. Cremar, D. Van Gough, S. L. Potisek, M. T. Ong, P. V. Braun, T. J. Martínez, S. R. White, J. S. Moore, and N. R. Sottos, Force-induced activation of covalent bonds in mechanoresponsive polymeric materials, Nature (London) **459**, 68 (2009).

[6] Y. Zhang, Z. Wang, T. B. Kouznetsova, Y. Sha, E. Xu, L. Shannahan, M. Fermen-Coker, Y. Lin, C. Tang, and S. L. Craig, Distal conformational locks on ferrocene mechanophores guide reaction pathways for increased mechanochemical reactivity, Nat. Chem. **13**, 56 (2021).

[7] Z. Chen, X. Zhu, J. Yang, J. A. M. Mercer, N. Z. Burns, T. J. Martinez, and Y. Xia, The cascade unzipping of ladderane reveals dynamic effects in mechanochemistry, Nat. Chem. **12**, 302 (2020).

[8] H. M. Klukovich, T. B. Kouznetsova, Z. S. Kean, J. M. Lenhardt, and S. L. Craig, A backbone lever-arm effect enhances polymer mechanochemistry, Nat. Chem. **5**, 110 (2013).

[9] B. W. Hamilton and A. Strachan, Rapid activation of non-oriented mechanophores via shock loading and spallation, Phys. Rev. Mater. **7**, 045601 (2023).

[10] B. A. Steele, N. Goldman, I. F. W. Kuo, and M. P. Kroonblawd, Mechanochemical synthesis of glycine oligomers in a virtual rotational diamond anvil cell, Chem. Sci. **11**, 7760 (2020).

[11] N. Goldman, E. J. Reed, L. E. Fried, I. F. William Kuo, and A. Maiti, Synthesis of glycine-containing complexes in impacts of comets on early earth, Nat. Chem. **2**, 949 (2010).

[12] J. J. Gilman, Chemical reactions at detonation fronts in solids, Philos. Mag. **71**, 1057 (1995).

[13] M. A. Wood, M. J. Cherukara, E. M. Kober, and A. Strachan, Ultrafast chemistry under nonequilibrium conditions and the shock to deflagration transition at the nanoscale, J. Phys. Chem. C **119**, 22008 (2015).

[14] M. P. Kroonblawd and L. E. Fried, High Explosive Ignition through Chemically Activated Nanoscale Shear Bands, Phys. Rev. Lett. **124**, 206002 (2020).

[15] B. W. Hamilton, M. P. Kroonblawd, and A. Strachan, Extemporaneous mechanochemistry: Shockwave induced ultrafast chemical reactions due to intramolecular strain energy, J. Phys. Chem. Lett. **13**, 6657 (2022).

[16] J. Ribas-Arino and D. Marx, Covalent mechanochemistry: Theoretical concepts and computational tools with applications to molecular nanomechanics, Chem. Rev. **112**, 5412 (2012).

[17] T. Friščić, I. Halasz, P. J. Beldon, A. M. Belenguer, F. Adams, S. A. J. Kimber, V. Honkimäki, and R. E. Dinnebier, Real-time and in situ monitoring of mechanochemical milling reactions, Nat. Chem. **5**, 66 (2013).

[18] M. Grandbois, M. Beyer, M. Rief, H. Clausen-Schaumann, and H. E. Gaub, How strong is a covalent bond? Science **283**, 1727 (1999).

[19] Z. Huang, Q. Z. Yang, D. Khvostichenko, T. J. Kucharski, J. Chen, and R. Boulatov, Method to derive restoring forces of

strained molecules from kinetic measurements, J. Am. Chem. Soc. **131**, 1407 (2009).
[20] M. T. Ong, J. Leiding, H. Tao, A. M. Virshup, and T. J. Martínez, First principles dynamics and minimum energy pathways for mechanochemical ring opening of cyclobutene, J. Am. Chem. Soc. **131**, 6377 (2009).
[21] T. Stauch and A. Dreuw, Knots "choke off" polymers upon stretching, Angew. Chem. Int. Ed. **55**, 811 (2016).
[22] A. M. Saitta and M. L. Klein, Evolution of fragments formed at the rupture of a knotted alkane molecule, J. Am. Chem. Soc. **121**, 11827 (1999).
[23] M. L. Mansfield, Knots in Hamilton cycles, Macromolecules **27**, 5924 (1994).
[24] A. M. Saitta, P. D. Soper, E. Wasserman, and M. L. Klein, Influence of a knot on the strength of a polymer strand, Nature (London) **399**, 46 (2019).
[25] T. Stauch, M. T. Hoffmann, and A. Dreuw, Spectroscopic monitoring of mechanical forces during protein folding by using molecular force probes, ChemPhysChem **17**, 1486 (2016).
[26] M. Paulsson, C. Krag, T. Frederiksen, and M. Brandbyge, Conductance of alkanedithiol single-molecule junctions: A molecular dynamics study, Nano Lett. **9**, 117 (2009).
[27] Y. Qi, J. Qin, G. Zhang, and T. Zhang, Breaking mechanism of single molecular junctions formed by octanedithiol molecules and Au electrodes, J. Am. Chem. Soc. **131**, 16418 (2009).
[28] P. Vélez, S. A. Dassie, and E. P. M. Leiva, First Principles Calculations of Mechanical Properties of 4,4′-Bipyridine Attached to Au Nanowires, Phys. Rev. Lett. **95**, 045503 (2005).
[29] C. Jarzynski, Nonequilibrium Equality for Free Energy Differences, Phys. Rev. Lett. **78**, 2690 (1997).
[30] C. Jarzynski, Equilibrium free-energy differences from nonequilibrium measurements: A master-equation approach, Phys. Rev. E **56**, 5018 (1997).
[31] S. Park and K. Schulten, Calculating potentials of mean force from steered molecular dynamics simulations, J. Chem. Phys. **120**, 5946 (2004).
[32] S. Park, F. Khalili-Araghi, E. Tajkhorshid, and K. Schulten, Free energy calculation from steered molecular dynamics simulations using Jarzynski's equality, J. Chem. Phys. **119**, 3559 (2003).
[33] B. Isralewitz, M. Gao, and K. Schulten, Steered molecular dynamics and mechanical functions of proteins, Curr. Opin. Struct. Biol. **11**, 224 (2001).
[34] M. K. Beyer, The mechanical strength of a covalent bond calculated by density functional theory, J. Chem. Phys. **112**, 7307 (2000).
[35] J. Ribas-Arino, M. Shiga, and D. Marx, Understanding covalent mechanochemistry, Angew. Chem. Int. Ed. **48**, 4190 (2009).
[36] K. Wolinski and J. Baker, Theoretical predictions of enforced structural changes in molecules, Mol. Phys. **107**, 2403 (2009).
[37] D. H. Ess and K. N. Houk, Distortion/interaction energy control of 1,3-dipolar cycloaddition reactivity, J. Am. Chem. Soc. **129**, 10646 (2007).
[38] D. H. Ess and K. N. Houk, Theory of 1,3-dipolar cycloadditions: Distortion/interaction and frontier molecular orbital models, J. Am. Chem. Soc. **130**, 10187 (2008).
[39] I. Fernández and F. M. Bickelhaupt, The activation strain model and molecular orbital theory: Understanding and designing chemical reactions, Chem. Soc. Rev. **43**, 4953 (2014).
[40] F. M. Bickelhaupt and K. N. Houk, Analyzing reaction rates with the distortion/interaction-activation strain model, Angew. Chem. Int. Ed. **56**, 10070 (2017).
[41] B. W. Hamilton and T. C. Germann, Energy localization efficiency in 1,3,5-trinitro-2,4,6-triaminobenzene pore collapse mechanisms, J. Appl. Phys. **133**, 035901 (2023).
[42] T. Stauch and A. Dreuw, Advances in quantum mechanochemistry: Electronic structure methods and force analysis, Chem. Rev. **116**, 14137 (2016).
[43] B. W. Hamilton, M. P. Kroonblawd, C. Li, and A. Strachan, A hotspot's better half: Non-equilibrium intra-molecular strain in shock physics, J. Phys. Chem. Lett. **12**, 2756 (2021).
[44] D. Guo, Q. An, W. A. Goddard, S. V. Zybin, and F. Huang, Compressive shear reactive molecular dynamics studies indicating that cocrystals of TNT/CL-20 decrease sensitivity, J. Phys. Chem. C **118**, 30202 (2014).
[45] M. P. Kroonblawd and N. Goldman, Mechanochemical formation of heterogeneous diamond structures during rapid uniaxial compression in graphite, Phys. Rev. B **97**, 184106 (2018).
[46] B. W. Hamilton and T. C. Germann, Interplay of mechanochemistry and material processes in the graphite to diamond phase transformation, arXiv:2302.04684 (2023).
[47] M. M. Islam and A. Strachan, Role of dynamical compressive and shear loading on hotspot criticality in RDX via reactive molecular dynamics, J. Appl. Phys. **128**, 065101 (2020).
[48] B. W. Hamilton, M. P. Krosonblawd, and A. Strachan, The potential energy hotspot: Effects from impact velocity, defect geometry, and crystallographic orientation, J. Phys. Chem. C **126**, 3743 (2022).
[49] B. W. Hamilton, M. P. Kroonblawd, J. Macatangay, H. K. Springer, and A. Strachan, Intergranular hotspots: A molecular dynamics study on the influence of compressive and shear work, J. Phys. Chem. C **127**, 9858 (2023).
[50] S. Plimpton, Fast parallel algorithms for short-range molecular dynamics, J. Comput. Phys. **117**, 1 (1995).
[51] A. P. Thompson, H. M. Aktulga, R. Berger, D. S. Bolintineanu, W. M. Brown, P. S. Crozier, P. J. in 't Veld, A. Kohlmeyer, S. G. Moore, T. D. Nguyen, R. Shan, M. J. Stevens, J. Tranchida, C. Trott, and S. J. Plimpton, LAMMPS - a flexible simulation tool for particle-based materials modeling at the atomic, meso, and continuum scales, Comput. Phys. Commun. **271**, 108171 (2022).
[52] See Supplemental Material at http://link.aps.org/supplemental/10.1103/PhysRevMaterials.7.075601 for additional method descriptions and results figures.
[53] A. C. T. Van Duin, S. Dasgupta, F. Lorant, and W. A. Goddard, ReaxFF: A reactive force field for hydrocarbons, J. Phys. Chem. A **105**, 9396 (2001).
[54] A. K. Rappé and W. A. Goddard, Charge equilibration for molecular dynamics simulations, J. Phys. Chem. **95**, 3358 (1991).
[55] H. H. Cady and A. C. Larson, The crystal structure of 1,3,5-triamino-2,4,6-trinitrobenzene, Acta Crystallogr. **18**, 485 (1965).
[56] M. A. Wood, D. E. Kittell, C. D. Yarrington, and A. P. Thompson, Multiscale modeling of shock wave localization in porous energetic material, Phys. Rev. B **97**, 014109 (2018).
[57] B. W. Hamilton, M. P. Kroonblawd, M. M. Islam, and A. Strachan, Sensitivity of the shock initiation threshold of

1,3,5-triamino-2,4,6-trinitrobenzene (TATB) to nuclear quantum effects, J. Phys. Chem. C **123**, 21969 (2019).

[58] B. W. Hamilton, B. A. Steele, M. N. Sakano, M. P. Kroonblawd, I. F. W. Kuo, and A. Strachan, Predicted reaction mechanisms, product speciation, kinetics, and detonation properties of the insensitive explosive 2,6-diamino-3, 5-dinitropyrazine-1-oxide (llm-105), J. Phys. Chem. A **125**, 1766 (2021).

[59] H. E. Kissinger, Variation of peak temperature with heating rate in differential thermal analysis, J. Res. Natl. Bur. Stand. **57**, 217 (1956).

[60] L. Liu, Y. Liu, S. V. Zybin, H. Sun, and W. A. Goddard, ReaxFF-lg: Correction of the ReaxFF reactive force field for London dispersion, with applications to the equations of state for energetic materials, J. Phys. Chem. A **115**, 11016 (2011).

[61] E. Polak and G. Ribiere, Note sur la convergence de méthodes de directions conjuguées, Revue française d'informatique et de recherche opérationnelle. Série rouge **3**, 35 (1969).

[62] B. W. Hamilton, M. N. Sakano, C. Li, and A. Strachan, Chemistry under shock conditions, Annu. Rev. Mater. Res. **51**, 101 (2021).

[63] M. Sakano, B. W. Hamilton, M. M. Islam, and A. Strachan, Role of molecular disorder on the reactivity of RDX, J. Phys. Chem. C **122**, 27032 (2018).

[64] M. P. Kroonblawd, B. W. Hamilton, and A. Strachan, Fourier-like thermal relaxation of nanoscale explosive hot spots, J. Phys. Chem. C **125**, 20570 (2021).

[65] G. I. Bell, Models for the specific adhesion of cells to cells, Science **200**, 618 (1978).

[66] G. S. Hammond, A correlation of reaction rates, J. Am. Chem. Soc. **77**, 334 (1955).

[67] R. P. Bell, The theory of reactions involving proton transfers, Proc. R. Soc. London, Ser. A: Math. Phys. Sci. **154**, 414 (1936).

[68] M. G. Evans and M. Polanyi, Further considerations on the thermodynamics of chemical equilibria and reaction rates, Trans. Faraday Soc. **32**, 1333 (1936).

[69] C. J. Wu and L. E. Fried, Ring closure mediated by intramolecular hydrogen transfer in the decomposition of a push-pull nitroaromatic: TATB, J. Phys. Chem. A **104**, 6447 (2000).

[70] https://petreldata.net/mdf/detail/mbsmd_v1.2.